JOURNAL OF GEOPHYSICAL RESEARCH, VOL. 94, NO. C7, PAGES 9731–9742, JULY 15, 1989

A Simple Analytical Formula to Compute Clear Sky Total and Photosynthetically Available Solar Irradiance at the Ocean Surface

ROBERT FROUIN, DAVID W. LINGNER, AND CATHERINE GAUTIER

California Space Institute, Scripps Institution of Oceanography, La Jolla

KAREN S. BAKER

Marine Bio-Optics, Scripps Institution of Oceanography, La Jolla, California

RAY C. SMITH

Marine Bio-Optics, University of California, Santa Barbara

A simple yet accurate analytical formula is proposed to compute total and photosynthetically available solar irradiance at the ocean surface under clear skies. The formula takes into account the most important processes occurring within the atmosphere, namely, scattering by molecules and aerosols and absorption by water vapor, ozone, and aerosols. These processes are parameterized as a function of solar zenith angle, aerosol type, atmospheric visibility, and vertically integrated water vapor and ozone amounts. When compared with the radiative transfer model of Tanré et al. (1979), the formula shows excellent agreement (to within 1%) under most atmospheric conditions and solar zenith angles. There is also good agreement with formulas developed by other investigators to estimate total solar irradiance. Comparisons of calculated and measured total and photosynthetically available solar irradiances for several experiments in both tropical and mid-latitude oceanic regions show 39 and 14 Wm^{-2} rms errors (6.5 and 4.7% of the average measured values) on an hourly time scale, respectively. The proposed formula is unique in its ability to predict surface solar irradiance in the photosynthetically active spectral interval. Furthermore, it may also be used for converting total irradiance measurements into photosynthetically available irradiance estimates. Combining the clear sky irradiance formula with satellite techniques to retrieve cloud effect on solar irradiance, pigment concentration, and sea surface temperature would provide useful primary productivity estimates over large oceanic areas and eventually the global oceans.

1. INTRODUCTION

The amount of solar irradiance reaching the ocean surface is important in both physical and biological oceanography. From the physical point of view, the incoming irradiance from the entire solar spectrum, or total solar irradiance, constitutes a major boundary forcing for oceanic circulation and acts as a crucial parameter for determining meridional heat transport. From the biological point of view, the solar irradiance in the photosynthetically active interval (350–700 nm), otherwise known as photosynthetically available radiation (PAR), regulates marine primary productivity and therefore the evolution of aquatic ecosystems.

Currently, models to predict upper ocean properties such as temperature and primary productivity use either shipboard measurements or climatological light levels as input. In situ measurements, generally confined to regions of research experiments, are sparse, while regional and seasonal averages, produced from meteorological data collected aboard ships of opportunity, are limited in both accuracy and coverage.

Interestingly, many models and formulas have been proposed for estimating total solar irradiance [e.g., *Kimball*, 1928; *Mosby*, 1936; *Laevastu*, 1960; *Berliand*, 1960; *Lumb*, 1964; *Atwater and Brown*, 1974; *Davies et al.*, 1975; *Reed*, 1977], but none for PAR. Until recently, most of the questions addressed in biological oceanography have involved space and time scales for which PAR can be directly measured. Furthermore, it has often proved satisfactory to take PAR as a more or less constant fraction of the total solar irradiance [e.g., *Jerlov*, 1974, 1976; *Jitts et al.*, 1976]. The relationship between PAR and total solar irradiance, however, depends upon atmospheric characteristics and radiation geometry [*Baker and Frouin*, 1987]. As interest in mapping primary productivity over large oceanic areas grows, an accurate, rapid estimate of PAR for various atmospheric conditions becomes essential.

A simple yet accurate analytical formula is presented here in order to permit computation from a few common input parameters of total solar irradiance and of PAR at the ocean surface under clear skies. The formula is founded upon the principles of radiative transfer and is verified against other formulas and models. A direct comparison of the formula's predictions with in situ measurements is presented as well. The effect of clouds on solar irradiance, although important, is not investigated here. This effect can be treated separately; in general, it is sufficient to multiply clear sky irradiance by cloud transmittance. Since techniques have been developed to estimate cloud transmittance from satellite measurements of the solar radiation that is reflected by

Paper number 89JC00598.
0148-0227/89/89JC-00598$05.00

the Earth-atmosphere system [e.g., *Hay and Hanson*, 1978; *Tarpley*, 1979; *Gautier et al.*, 1980; *Dedieu et al.*, 1987], one could use a clear sky formula in conjunction with these techniques to provide an estimate of solar irradiance regardless of cloud conditions. So far, this approach has been investigated for total solar irradiance but not for PAR. Estimating PAR from satellite data is work currently in progress.

2. Derivation of the Analytical Formula

In the spectral range of interest, 250–4000 nm, solar radiation is scattered by air molecules and aerosols and is absorbed primarily by ozone, water vapor, carbon dioxide, oxygen, and aerosols. Scattering and absorption processes interact in a complicated manner, but fortunately, gaseous absorption can be treated separately. Qualitatively, the arguments are as follows. First, the ozone layer, located at high altitudes (30–40 km) where molecules are rarified, is traversed almost without scattering. Second, absorption by water vapor and carbon dioxide occurs mostly at wavelengths above 850 nm, where scattering is essentially due to aerosols. Since the aerosol phase function presents a predominantly forward peak, the photons at those wavelengths follow practically a direct path through the atmosphere. To account for ozone, water vapor, and carbon dioxide absorption, it is therefore sufficient to multiply the incoming irradiance by the transmittance of the respective gases along the direct path from the sun to the surface. Although such a treatment is more difficult to justify for oxygen absorption because molecular scattering is not negligible around 750 nm, it constitutes nonetheless a good approximation because oxygen absorption is very localized spectrally and the spectral intervals considered (the PAR range and the total solar spectrum) are comparatively wide. A more complete justification of decoupling gaseous absorption and scattering is given by *Deschamps et al.* [1983] and *Tanré et al.* [1985]. Neglecting the thermal emission of the atmosphere, and assuming that the surface is Lambertian and uniform, one can write the irradiance reaching the surface in the wavelength range λ_1–λ_2 from the sun at zenith angle θ as:

$$I_{\lambda_1-\lambda_2}(\theta) \simeq \int_{\lambda_1}^{\lambda_2} I_{0\lambda}\,(d/d_0)^2 \cdot \cos\,\theta \exp\frac{(-\tau_\lambda/\cos\,\theta) + t_{d\lambda}(\theta)}{1 - r_\lambda(\theta)s_\lambda}\, t_{g\lambda}(\theta)\, d\lambda \qquad (1)$$

where $I_{0\lambda}$ is the monochromatic extraterrestrial solar irradiance, d/d_0 is the ratio of actual to mean Earth-Sun separation, τ_λ is the optical thickness (or turbidity) of the atmosphere, r_λ is the surface reflectance, $t_{d\lambda}$ is the diffuse sky transmittance, $t_{g\lambda}$ is the transmittance due to absorbing gases, and s_λ is the spherical albedo of the atmosphere. In this expression, $\exp(-\tau_\lambda/\cos\theta)$ represents direct solar beam attenuation and $1 - r_\lambda s_\lambda$ accounts for photons that have experienced one or multiple surface reflections. The assumption of a Lambertian and uniform surface is not actually verified (r_λ depends on solar zenith angle, surface roughness, and water type) but remains reasonable because $r_\lambda s_\lambda$ is generally small (<0.05). In the presence of sun glint, however, $r_\lambda s_\lambda$ reaches much higher values, and neglecting the bidirectional properties of r_λ introduces nonnegligible errors.

According to *Tanré et al.* [1979], $t_{d\lambda}$ and s_λ can be expressed with good approximation as

$$t_{d\lambda} \simeq \exp-[(\alpha\tau_{r\lambda}+\beta_\lambda\tau_{a\lambda})/\cos\,\theta] - \exp\,(-\tau_\lambda/\cos\,\theta) \qquad (2)$$

$$s_\lambda \simeq (\alpha'\tau_{r\lambda} + B'_\lambda\tau_a\lambda)(\exp\,(-\tau_\lambda) \qquad (3)$$

where $\tau_{r\lambda}$ and $\tau_{a\lambda}$ are Rayleigh and aerosol optical thicknesses, respectively; $\tau_\lambda = \tau_{r\lambda} + \tau_{a\lambda}$; and α, β, α', and β'_λ are coefficients that are either constant (α, α') or dependent on wavelength for a particular aerosol type (β_λ, β'_λ). Since $\tau_{a\lambda}$ is generally not measured, surface visibility, a parameter routinely observed aboard ships, may be used instead. One should bear in mind, however, that the relationship between $\tau_{a\lambda}$ and surface visibility is only a rough inverse proportionality. Stratospheric aerosols, for instance, would not affect surface visibility.

Strictly speaking, $t_{g\lambda}$, unlike $t_{d\lambda}$ and s_λ, cannot be expressed monochromatically because gaseous absorption varies much too rapidly with wavelength (line spectrum). We therefore define $t_{g\lambda}$ as the average transmittance over a sufficiently large spectral interval (typically 5 nm) centered at λ. With such a definition, the transmittance function for each absorbing gas i can be modeled accurately as

$$t_{i\lambda} \simeq \exp\,[-\alpha_{i\lambda}(U_i^*\cos\,\theta)^{\beta_{i\lambda}}] \qquad (4)$$

where U_i^* is a vertically integrated absorber amount, suitably scaled to account for the temperature and pressure dependence of absorption, and $\alpha_{i\lambda}$ and $\beta_{i\lambda}$ are coefficients derived from experimental measurements or calculated theoretically. According to theory [e.g., *Goody*, 1964], $\beta_{i\lambda}$ takes values between 0.5 (strong absorption regime) and 1 (weak absorption regime). For a gas located mainly in the lower troposphere, such as water vapor, U_i^* is nearly equal to the actual total (vertically integrated) absorber amount U_i. This is not the case for ozone, carbon dioxide, and oxygen, but the influence of these gases is so weak in the spectral intervals considered that we can still express their transmittance fairly accurately as an explicit function of U_i instead of U_i^*. We shall therefore write

$$t_{g\lambda} = \prod_i t_{i\lambda} \simeq \prod_i \exp\,[-\alpha'_{i\lambda}(U_i/\cos\,\theta)^{\beta'_{i\lambda}}] \qquad (5)$$

where $\alpha'_{i\lambda}$ and $\beta'_{i\lambda}$ are adjusted coefficients.

The previous considerations lead to the following analytical formula for $I_{\lambda_1-\lambda_2}$:

$$I_{\lambda_1-\lambda_2} \simeq I_{0\lambda_1-\lambda_2}\,(d/d_0)^2 \cdot \cos\,\theta \frac{\exp\,[-(a + b/V)/\cos\,\theta]}{1 - \bar{r}_{\lambda_1-\lambda_2}(a' + b'/V)} \cdot \exp\,[-a_v(U_v/\cos\,\theta)^{b_v}] \cdot \exp\,[-a_o(U_o/\cos\,\theta)^{b_o}] \qquad (6)$$

where $I_{0\lambda_1-\lambda_2}$ is the monochromatic extraterrestrial irradiance integrated over λ_1–λ_2, $\bar{r}_{\lambda_1-\lambda_2}$ is the average surface reflectance over λ_1–λ_2, V is surface visibility, subscripts v and o denote water vapor and ozone, respectively, and a, a', b, b', a_v, b_v, a_o, and b_o are coefficients to be determined. These coefficients depend on the spectral interval λ_1–λ_2 considered. Some of them, namely a, a', b, and b', also vary with aerosol type. In (6), absorption by carbon dioxide and

TABLE 1. Top-of-Atmosphere Solar Irradiance in the Spectral Intervals Considered

Spectral Interval, nm	Solar Irradiance, W m^{-2}
350–700	584.9 (43%)
400–700	531.2 (39%)
250–4000	1358.2 (100%)

oxygen is not explicitly parameterized but is implicitly taken into account in the coefficient a, since the concentration of these gases is fairly constant (to simplify, we further assume $\beta'_{i\lambda} = 1$). Note also that the term multiplying $\bar{r}_{\lambda_1-\lambda_2}$ should involve higher orders of $1/V$ because exp $(-\tau_\lambda)$ appears in (3), but first-order development is justified because $r_\lambda s_\lambda$ is generally small.

To determine the various coefficients of (6), a wide range of atmospheric and geometric conditions are considered, namely surface visibilities from 5 to 100 km, total water vapor amounts from 0.5 to 5 g cm^{-2}, total ozone amounts from 0.1 to 0.5 atm cm (100 to 500 Dobson units; 1 DU $= 2.69 \times 10^{16}$ molecules O_3 cm^{-2}) and solar zenith angles from 0° to 80°. For these conditions, $I_{\lambda_1-\lambda_2}$ is first computed using Tanré et al.'s radiative transfer model. In the calculations, $I_{0\lambda}$ is taken from *Neckel and Labs* [1984] and r_λ is taken from *Viollier* [1980]. The model of Tanré et al. has not been validated by direct measurements, but its predictions do not differ from exact calculations by more than 1%, except at solar zenith angles greater than 80° [e.g., *Duhaut*, 1985]. Such angles are not discussed owing to the limited accuracy of Tanré's et al. model at large solar zenith angles. By inserting calculated irradiances and corresponding input parameters in (6), the analytical formula's coefficients are obtained by regression.

The eight coefficients are determined for three spectral intervals and two aerosol models. The spectral intervals are 250–4000 nm, representing virtually the total solar spectrum; 350–700 nm, the officially defined PAR range; and 400–700 nm, the band for which modern instruments measure PAR. Table 1 displays the top-of-atmosphere solar irradiance in each of these intervals. About 43% of the total solar irradiance originates from wavelengths within the interval 350–700 nm, and 39% originates from wavelengths of 400–700 nm. Even though only 99% of the extraterrestrial solar irradiance is confined to wavelengths between 250 and 4000 nm, using 1358.2 W m^{-2} instead of the solar constant (1372 W m^{-2}, after *Neckel and Labs* [1984]) for $I_{0\lambda_1-\lambda_2}$ in the total solar spectrum is justified since practically no solar energy traverses the atmosphere outside the 250- to 4000-nm range. The aerosol models, selected from those proposed by the International Radiation Commission [*World Climate Program*, 1983], correspond to typical maritime and continental aerosols. The maritime model consists mostly of a spectrally white and little-absorbing component, whereas the continental model is a spectrally red and more absorbing mixture of about 70% dustlike and 30% water-soluble components.

Table 2 gives the coefficients obtained for the three spectral intervals and the two aerosol models when V is expressed in kilometers, U_v in grams per square centimeter, and U_o in atm-cm. The coefficient b exhibits higher values in the short-wavelength intervals owing to the higher extinction cross section, σ, in these intervals. For maritime aerosols, b has nearly the same value in the intervals 350–700 nm and 400–700 nm owing to the weak wavelength dependence of σ and the coefficient β in (2) (β increases linearly as the anisotropy factor of the phase function decreases). In all spectral intervals, b is lower for maritime aerosols. This is not quite expected in the 250- to 4000-nm interval, since σ is higher for maritime aerosols; here, the effect of a lower β dominates. The same type of argument explains the variations of b', except that these now follow the variations of σ, even in the 250- to 4000-nm interval. Since aerosols affect atmospheric visibility only above a minimum concentration that depends on aerosol type, a and a' are not constant for maritime and continental aerosols. As expected, a_v is extremely low in the intervals 350–700 nm and 400–700 nm because water absorbs only weakly in the so-called "rain" bands between 570 and 700 nm; a_v is much higher (by 2.5 orders of magnitude) in the 250- to 4000-nm interval. Unlike a_v, b_v is much lower in the 250- to 4000-nm interval, a direct consequence of the strong water vapor absorption regime in the infrared. The small a_v values in the short-wavelength intervals suggest that water vapor absorption need not be included in our formula (in the moistest conditions and with the sun at zenith, neglecting water would result in at most a 1% overestimation of irradiance). Because of the large effect of water vapor upon the total irradiance, we have included the term in our formula for generality. As expected, a_o and b_o exhibit their lowest values in the interval 250–4000 nm (ozone absorption occurs below 390 nm and in the Chapuis bands around 600 nm). Moreover, since the peak of ozone absorption in the visible is closer to the red end of the spectrum than to the violet end, a_o is lower in the 350- to 700-nm interval than in the 400- to 700-nm interval. The lower b_o values in the 250- to 4000-nm interval are a manifestation of the strong ozone absorption regime below 290 nm.

Figure 1 shows the performance of the analytical formula when compared against the *Tanré et al.* [1979] model. Only the results for the 400- to 700-nm and 250- to 4000-nm intervals are presented, since those for the 350- to 700-nm interval are quite similar to the former. In the comparison, we use the US62 standard atmosphere of *McClatchey* [1972], characterized by a 1.4 g cm^{-2} total water vapor amount and a 0.34 atm cm total ozone amount, and consider two surface visibilities, namely 23

TABLE 2. Regression Coefficients for Analytical Formula

Spectral Interval, nm	Aerosol Type	a	b	a'	b'	a_v	b_v	a_o	b_o
350–700	maritime	0.079	0.378	0.132	0.470	0.002	0.87	0.047	0.99
	continental	0.089	0.906	0.138	0.576	0.002	0.87	0.047	0.99
400–700	maritime	0.068	0.379	0.117	0.493	0.002	0.87	0.052	0.99
	continental	0.078	0.882	0.123	0.594	0.002	0.87	0.052	0.99
250–4000	maritime	0.059	0.359	0.089	0.503	0.102	0.29	0.041	0.57
	continental	0.066	0.704	0.088	0.456	0.102	0.29	0.041	0.57

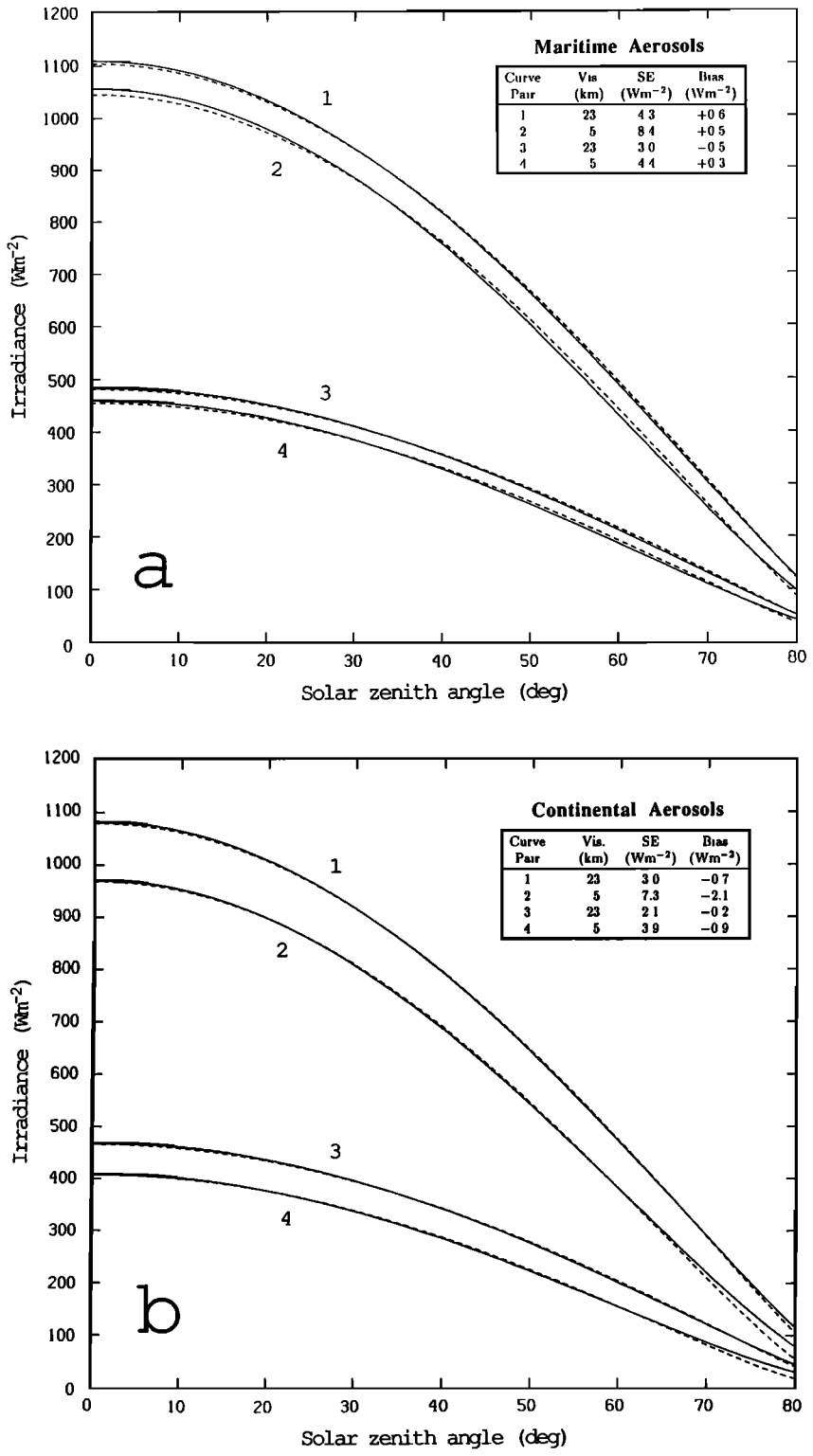

Fig. 1. Comparisons of I_{PAR} and I_{tot} for (*a*) maritime and (*b*) continental aerosols as predicted by the model of *Tanré et al.* [1979] (solid line) and the analytical formula presented herein (dashed line). The top two curve pairs (1 and 2) are I_{tot}; the bottom two (3 and 4) are I_{PAR}.

and 5 km. The agreement between our formula and Tanré et al.'s model is generally very good and is best when the aerosols are continental and the visibility is equal to 23 km. For maritime aerosols, the formula underestimates solar irradiance at solar zenith angles below 30° and overestimates solar irradiance at solar zenith angles above 40°. Still, the differences are not more than 2% in either spectral interval, even at large solar zenith angles. For continental aerosols, the relative difference between the two models does not exceed 1% in either spectral interval, except at large solar zenith angles ($\theta > 75°$) and 5-km visibility, in which case the difference reaches a maximum of 4%. One notices in Figure 1 that surface visibility has more effect on solar irradiance when the atmosphere contains continental aerosols.

Since it is often total solar irradiance and not PAR that is measured on board ships, we have also examined the performance of our formula in predicting the ratios $I_{350-700}/I_{250-4000}$ and $I_{400-700}/I_{250-4000}$. Knowing these ratios gives access to a PAR estimate from a total solar irradiance measurement. Comparisons with Tanré et al.'s model (not shown here) indicate that for most atmospheric conditions and a sun within 70° of zenith, the agreement is better than 0.5%. For solar zenith angles above 70°, the agreement is not as good; differences of up to 5% exist between the two types of prediction (overestimation of our formula), which reflect our formula's much larger underestimation of $I_{250-4000}$ than $I_{400-700}$.

3. Comparison With Other Formulas

Among the various formulas that have been proposed to estimate total solar irradiance at the ocean surface, only those of *Lumb* [1964], *Atwater and Brown* [1974], and *Davies et al.* [1975] involve instantaneous radiation geometry. The other formulas, developed to compute daily integrals of solar irradiance directly, do not explicitly account for solar zenith angle variations during the course of the day. Rather, they use the average solar zenith angle during daylight hours or, alternatively, the noon solar zenith angle. In this section our formula is compared with the three more detailed models which use the instantaneous radiation geometry.

Lumb developed his formula from surface radiation data collected aboard the stationary weather ship *Juliett* (52°30'N, 20°W). He found experimental evidence that under virtually clear skies, the ratio $I_{tot}/S \cos\theta$, where the subscript "tot" refers to the entire solar spectrum and S is the solar constant, is a linear function of $\cos\theta$. This led to the following formula:

$$I_{tot} = S \cos\theta(a + b \cos\theta) \tag{7}$$

where a and b are determined by a least squares fit. Taking $S = 1350$ W m^{-2}, Lumb found $a = 0.61$ and $b = 0.2$. Atmospheric absorption and scattering processes are not parameterized in (7); the formula only reflects average atmospheric conditions at *Juliett*'s location. Lumb's formula, however, has subsequently proven satisfactory in other oceanic areas [e.g., *Simpson and Paulson*, 1979; *Lind et al.*, 1984]. This is not surprising, in fact, because the solar zenith angle is the most influential parameter on the clear sky solar irradiance reaching the surface and it can be calculated exactly.

Unlike Lumb's formula, *Atwater and Brown*'s [1974] formula is based on theoretical considerations. In clear sky conditions, the incoming solar flux is written as

$$I_{tot} = S \cos\theta P(G - A) \tag{8}$$

where P is the transmittance for aerosol scattering and absorption, A is the absorptance of water vapor, and G is the transmittance for molecular scattering and absorption by other gases (including ozone). The functions P, G, and A are defined as

$$P = \exp\left(\frac{-\tau_c p}{1013 \cos\theta}\right) \tag{9}$$

$$G = 0.485 + 0.515\left[1.041 - 0.16\left(\frac{0.000949p + 0.051}{\cos\theta}\right)^{0.5}\right] \tag{10}$$

$$A = 0.077(U_v/\cos\theta)^{0.3} \tag{11}$$

where p is the surface pressure in millibars and τ_c characterizes aerosol opacity. In (11), U_v is expressed in grams per square centimeter. The essential physics of the problem are thus accounted for in (8), although no ozone variations are permitted. The formula takes into account the effect of pressure on atmospheric optical thickness, a feature that does not appear in our formula. This effect is secondary but could be easily introduced, at least approximately, by multiplying the term $a + b/V$ in (6) by $p/1013$. One notices in (8) that the water vapor absorptance is subtracted from the transmittance of the dry, hazeless atmosphere. This procedure is not satisfactory because it implies that $G - A$ can be negative. In fact, the transmittance of the moist, hazeless atmosphere is more appropriately expressed as $G(1 - A)$. Since A is relatively small, using $G - A$ instead of $G(1 - A)$, although conceptually incorrect, has no noticeable effect. Examining (10) and (11), one also notices that G can be negative and A greater than 1 when the sun is near the horizon. In that case, the optical air mass ($1/\cos\theta$) should be modified to account for atmospheric refraction.

Finally, in *Davies et al.*'s [1975] formula the solar irradiance reaching the surface is expressed as

$$I_{tot} = S \cos\theta \psi_{wa}\psi_{da}(\psi_{ws}\psi_{rs}\psi_{ds} + 1)/2 \tag{12}$$

where ψ_{wa}, ψ_{da}, ψ_{ws}, ψ_{rs}, and ψ_{ds} are transmission functions for water vapor absorption, aerosol absorption, water vapor scattering, Rayleigh scattering, and aerosol scattering, respectively. It is assumed in (12) that direct solar radiation is absorbed before being scattered, that half of the scattered radiation reaches the surface, and that aerosol attenuation is due equally to absorption and scattering. In addition, ozone absorption is neglected. Scattering by water vapor is considered separately from scattering by other molecules, which allows one to take into account the effect of changes in molecular density (due mainly to water vapor) on the scattering cross section. The transmission functions are given by

$$\psi_{ws} = 1 - 0.0225U_v m \tag{13}$$

$$\psi_{rs} = 0.972 - 0.08262m + 0.00933m^2 - 0.00095m^3 + 0.0000437m^4 \tag{14}$$

$$\psi_{wa} = 1 - 0.077(U_v m)^{0.3} \tag{15}$$

$$\psi_{ds} = \psi_{da} = k^{m/2} \tag{16}$$

with

$$m = [\cos\theta + 0.15(93.885 - \theta)^{-1.253}]^{-1} \tag{17}$$

where m is air mass, k is a coefficient that depends on aerosol type and loading ($k < 1$), and U_v is expressed in grams per square centimeter. Note that the Davies et al. formula, as well as that of Atwater and Brown, does not take into account interactions between the photons and the sea surface.

For the comparisons to be meaningful, it is indeed important that the same atmospheric conditions and solar zenith angles be considered for all formulas. Unfortunately, the aerosol input parameters are different from one formula to the next. We must therefore determine exactly how they correspond. This is done by equating each formula's terms that describe the aerosol effect. Neglecting the photons'

multiple interactions with the sea surface in our formula, assuming p = 1013 mbar in Atwater and Brown's formula, and approximating m by 1/cos θ in Davies et al.'s formula, we obtain

$$k = \left\{ -0.5 + \left[0.25 + 2 \exp\left(-\left(a_a + \frac{b}{V} \right) \div \cos\theta \right) \right]^{1/2} \right\}^{2\cos\theta} \quad (18)$$

$$\tau_c = a_a + \frac{b}{V} \quad (19)$$

where a_a corresponds to the aerosol particles that do not affect the surface visibility ($a_a < a$). The coefficient a_a takes the values 0.025 and 0.012 when the aerosols are continental and maritime, respectively. We see in (18) that k is a function of θ. The dependence, however, is slight (k varies less than 1% when θ varies from 0° to 80°). For each turbid atmosphere selected, we therefore fix k at its average value over the θ range 0°–80°.

Figure 2 shows the formulas' predictions for a US62 atmosphere with 23-km visibility and containing either continental or maritime aerosols. The agreement between formulas is generally good. Maximum differences of 60 and 30 W m^{-2} are observed for maritime and continental aerosols, respectively. The predictions of the Atwater and Brown and Davies et al. formulas agree within 3–4 W m^{-2} at all solar zenith angles, but yield values higher than those of our formula by 20–25 W m^{-2} depending on the type of aerosols (larger bias with maritime aerosols). Lumb's formula gives the best agreement with our formula for continental aerosols. In this case the differences do not exceed 1% at solar zenith angles less than 60°, but they reach 15% at larger solar zenith angles. It is interesting to note that turbidity measurements made at Lages, Azores (38°N, 27°W), a location not too far from *Juliett* where Lumb's formula was established, have shown that the aerosol optical thickness in that region varies spectrally with an annually averaged Ångström exponent of 0.93 ± 0.3 [*Environmental Data Service*, 1977], which is more characteristic of continental aerosols than of maritime aerosols. Since the amount of solar radiation reaching the surface decreases as the atmospheric visibility decreases, Lumb's formula, which does not allow for aerosol loading variations, predicts higher solar irradiance values than does our formula at visibilities less than 23 km. In 5-km visibility conditions, for instance, the overestimation may reach 100 W m^{-2}.

4. In Situ Comparisons

The predictive power of (6) for I_{PAR} and I_{tot} has been tested against five separate ground truth data sets. Two of the experiments contain independent measurements of I_{tot} and I_{PAR}, thus providing an good validation situation. These two experiments were (1) the first Biowatt field experiment aboard the R/V *Knorr* in the Sargasso Sea (24°–35°N, 70°W) during April 12–22, 1985 [*Dickey et al.*, 1986], and (2) measurements taken at the Scripps Institution of Oceanography (SIO) pier (33°N, 117°W) during April 12 to May 10, 1984, in support of other bio-optical experiments at a nearby underwater mooring [*Booth et al.*, 1987]. The other three data sets contain I_{tot} data and no I_{PAR} data. These were (3) the Mixed Layer Dynamics Experiment (MILDEX), measurements of I_{tot} having been taken aboard R/P *FLIP* (Floating Instrument Platform) off Point Conception, California (34°N, 126°W), during October 26 to November 12, 1983 [*Lind and Katsaros*, 1987]; (4) the Tropic Heat experiment, comprising I_{tot} measurements from the R/V *Wecoma* in the tropical Pacific Ocean (3°S to 6°N, 140°W) during November 15 to December 4, 1983 [*Niiler*, 1987]; and (5) the Frontal Air-Sea Interaction Experiment (FASINEX), in which I_{tot} were measured from five surface moorings located southwest of Bermuda (27°N, 70°W) during February 5 to March 7, 1986 [*Pennington and Weller*, 1986].

Each of the five data sets was culled to eliminate all but clear sky measurements, as indicated ideally from direct observations of sky conditions. Cloud coverage data were available for MILDEX and for a subset of the SIO pier data set. The remaining data (SIO pier, Biowatt, FASINEX, and Tropic Heat) contained no cloud information. Therefore irradiance-time plots, constructed from the original data, were evaluated to determine the likely sky state. Only those time segments that were smooth and approximated a cosine relationship were included among the clear sky data.

The analytical formula (6) for I_{tot} and I_{PAR} requires six input parameters, two of which (the solar zenith angle and the ratio of the actual Earth-Sun distance to its annual mean) are known or can be computed from time and position data. The other four input parameters are aerosol type, visibility, and the vertically integrated concentrations of water vapor and ozone in the atmosphere. If not measured directly, these parameters can be estimated using monthly or seasonal climatological averages or indirect observational data.

The selection of the aerosol model was based upon wind velocity data from either the daily weather maps [e.g., *NOAA*, 1984] or monthly average vector mean wind barbs and direction frequency diagrams from the U.S. Navy marine climatic atlases of the world [e.g., *Meserve*, 1974]. Prevailing winds from a direction in which there is a nearby land mass are assumed to carry aerosols of continental origin; while those winds from predominantly oceanic regimes would convey maritime aerosols. The visibility was estimated from monthly average cumulative percent frequency diagrams in the Navy climatic atlases. Seasonal maps of mean concentrations and root-mean-square deviations of water vapor over the oceans, based upon 3 years (1979–1981) of remote sensing data from the Nimbus 7 scanning multichannel microwave radiometer (SMMR), plotted by *Prabhakara et al.* [1985], were used to estimate total water vapor amount. Finally, latitude-time plots of total ozone compiled by *Dutsch* [1969] from 3 years of International Geophysical Year and International Geophysical Committee data were used to determine monthly average vertically integrated atmospheric ozone concentrations. Table 3 lists average climatological values of the four parameters for the time of each experiment.

During the Biowatt cruise, a Biospherical Instruments spectroradiometer [*Smith et al.*, 1984] measured spectral downwelling irradiance above the ocean surface in 12 channels each having 10-nm half bandwidths and together spanning the wavelength range from 410 to 769 nm. The instrument was calibrated against a standard lamp, and the PAR irradiance was calculated by integrating the spectral data from 400 to 700 nm. The total irradiance was measured using an Eppley precision spectral pyranometer (model PSP) with

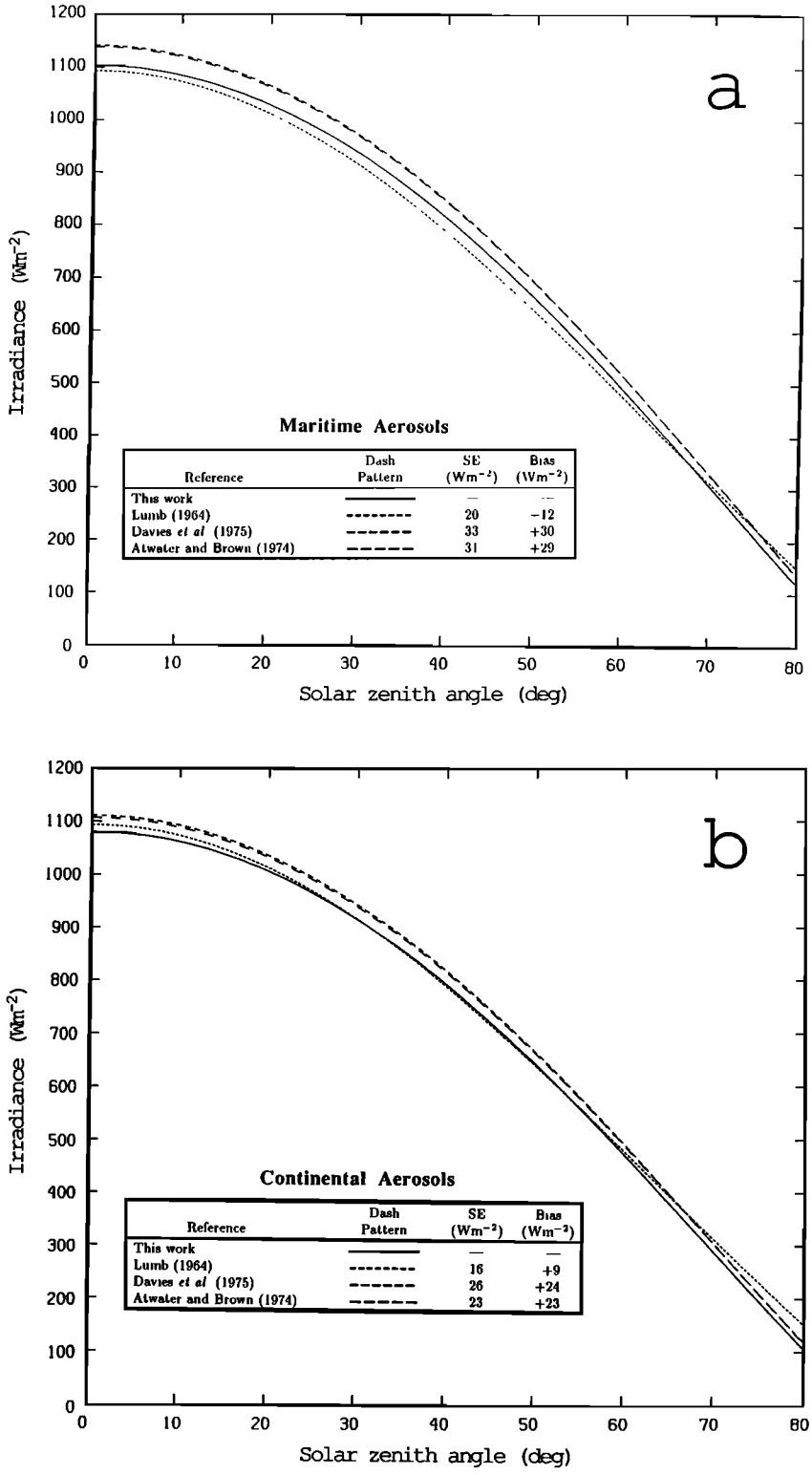

Fig. 2. Comparisons of various formulas that predict I_{tot}.

a WG7 clear glass cover transparent between 285 and 2800 nm. This pyranometer was calibrated against the entire solar spectrum [*Hill et al.*, 1966] and has a precision of ±2%. Both instruments were located on the ship's flying bridge, approximately 4 m from a reflective stack and 15 m above the sea surface. Although the location for the instruments was selected to minimize exposure errors, contamination due to ship structure both obscuring part of and reflecting into the fields of view may affect nominal precision figures by a few percent. The instruments were ungimbaled, which may further degrade the nominal precision, especially in the case of a preferential tilt of the ship [*Katsaros and DeVault*, 1986]. The Biowatt data represent 5-min averages and cover solar zenith angles from 14° to 70°.

For the SIO pier experiment, I_{PAR} was measured using a Biospherical Instruments cosine PAR sensor, calibrated

TABLE 3. Climatological Data for Each Individual Data Set

Data Set	Aerosol Model	Visibility, km	Water Vapor Amount, g cm^{-2}	Ozone Amount, atm cm
Biowatt	continental	27	2.5	0.31
SIO pier	maritime	25	1.8	0.32
MILDEX	maritime	30	2.0	0.28
Tropic Heat	maritime	31	4.0	0.25
FASINEX	continental	35	2.8	0.30

against a standard lamp. The total irradiance, I_{tot}, was measured using the same Eppley precision spectral pyranometer that was used during Biowatt. The two instruments were mounted side by side on a temporary wooden structure above the trailer at the end of the old SIO pier where there would be minimal obstruction from or reflection into the instruments' fields of view. The SIO pier data set comprises 22 sets of I_{PAR} and I_{tot} data with frequencies ranging from 0.2 to 15 min^{-1} and durations from 13 min to 3.5 days. These data were averaged over 30-min time intervals that had been designated clear by one of the above criteria.

The total irradiance data from the FASINEX were taken using Eppley pyranometers (model 8-48) placed atop each of five surface buoys. The pyranometers were calibrated with a precision of 5%. Buoy motion, however, is likely to increase this figure. The data were averages of 64 samples per 450 s [*Pennington and Weller*, 1986], later combined into 30-min averages which were used for this study.

For Tropic Heat, I_{tot} was measured from R/V *Wecoma* using a gimbal-mounted Eppley pyranometer (model 8-48), calibrated to factory specifications. The data are hourly averages of measurements taken at 2-min intervals (C. Paulson, Oregon State University, personal communication, 1987).

For MILDEX, a gimbal-mounted Eppley precision spectral pyranometer, model PSP, measured I_{tot} from R/P *FLIP* with only a few support wires within the immediate field of view of the instrument. The pyranometer was calibrated with an instrument error of 2% and an exposure error of 1%, resulting in a total precision of 2% for a single data sample. Individual samples (4 s^{-1}) were block averaged over 32-s periods, then smoothed and combined into 30-min averages for analysis [*Lind and Katsaros*, 1987].

Figure 3*a* shows predicted I_{PAR} plotted against measured I_{PAR} for the combined Biowatt and SIO pier data sets. Figure 3*b* shows predicted versus measured I_{tot} for all five experiments. Goodness of fit statistics for the combined data sets are noted in Figures 3*a* and 3*b*; those for the individual experiments are listed in Table 4.

For the combined data set, the calculated I_{PAR} values fit the surface data very well. The standard error (rms deviation) of the fit is 14 W m^{-2}, or 4.7% of a nominal mean of 300 W m^{-2}, and the bias (average deviation) is -5 W m^{-2} (negative bias indicates that predicted values are, on average, lower than measured data). Individually, the goodness of fit statistics for I_{PAR} are similar for both the Biowatt and the SIO pier comparisons. The standard error for each of the two experiments is between 10 and 20 W m^{-2}, and the biases both indicate an underestimation by the formula of about 5 W m^{-2} in I_{PAR}.

For total irradiance, calculated values and in situ data from the combined five experiments differ by an average of +8 W m^{-2}, indicating a slight overestimation of the data by the analytical formula. The standard error of the fit is 39 W m^{-2}, or 6.5% of a nominal mean of 600 W m^{-2}.

The overall good agreement between predicted and measured I_{tot} may be attributed mainly to the relative abundance of data (72% of all points) within the FASINEX data set. The biases for the five buoys range from +11 to −14 W m^{-2}, and the overall FASINEX bias is +1 W m^{-2}. The individual statistics for the other four experiments exhibit biases within the range 20–30 W m^{-2}, averaging +25 W m^{-2}. So, with the one exception, (6) tends to overestimate the total irradiance by 3–4% while underestimating I_{par} by around 2%.

In fact, one might argue that the FASINEX data are not an exception. If the maritime aerosol model were used in the prediction and the other three parameters input as listed in Table 3, then the bias would be +17 W m^{-2}, not +1 W m^{-2}, for the combined FASINEX data. The continental aerosol model was chosen for FASINEX on the basis of wind vector data [*Meserve*, 1974] showing westerly winds at 2.2 knots (1.1 m s^{-1}) on maps for both February and March at station "34" (30°N, 70°W). A look at the wind direction frequency diagram [*Meserve*, 1974], in fact, shows a scalar mean wind speed of 13.8 knots (7.1 m s^{-1}) spread evenly among the eight major compass points, indicating that assignment of the maritime aerosol model would not be totally improper. In this case, all five data sets would exhibit biases between +17 and +29 W m^{-2} for the prediction of total irradiance. Standard surface pressure maps and nearby station data for the specific days of buoy deployment [*NOAA*, 1985], however, justify our choice of continental aerosols. Still, the apparent reproducibility of the overprediction in most data sets must be addressed.

One possibility is overestimation of atmospheric transmittance by the *Tanré et al.* [1979] model. Comparisons with exact calculations [*Duhaut*, 1985] indicate that part of the discrepancy might originate from decoupling of gaseous absorption and scattering processes. Correcting for the resulting errors, however, would yield I_{tot} values lower by less than 1% for $\theta_s < 60°$. Thus model errors do not completely explain the observations. Another possible route to overprediction might be inadequate cloud screening of the original irradiance data. If some actually cloudy days had been included within the clear day data set, then some of the irradiance predicted by the clear sky model might have been blocked by those clouds, and the measured irradiance values would have been lower. The attenuation, however, would have affected both the I_{tot} and I_{PAR} measurements, although clouds are more transparent in the visible. In any case, the similarity in standard errors for all five I_{tot} prediction data sets (30–50 W m^{-2}) suggests that the cloud screening methods used were comparable, if not adequate. A third possible explanation might be measurement or calibration error. The 3–4% bias observed in the I_{tot} predictions of some data sets is close in magnitude to the precisions quoted for each pyranometer, but there is nothing to indicate any shortcomings in the accuracy of the instruments.

Aside from model errors and measurement and sampling errors, the positive bias for the I_{tot} predictions might yet be explained by the possibility that one or more of the input parameters for the formula may have been significantly different from the climatological averages used in the calculations. Table 5 shows the sensitivity of I_{PAR} and I_{tot} to the input parameters for standard atmospheric conditions. A 1 g

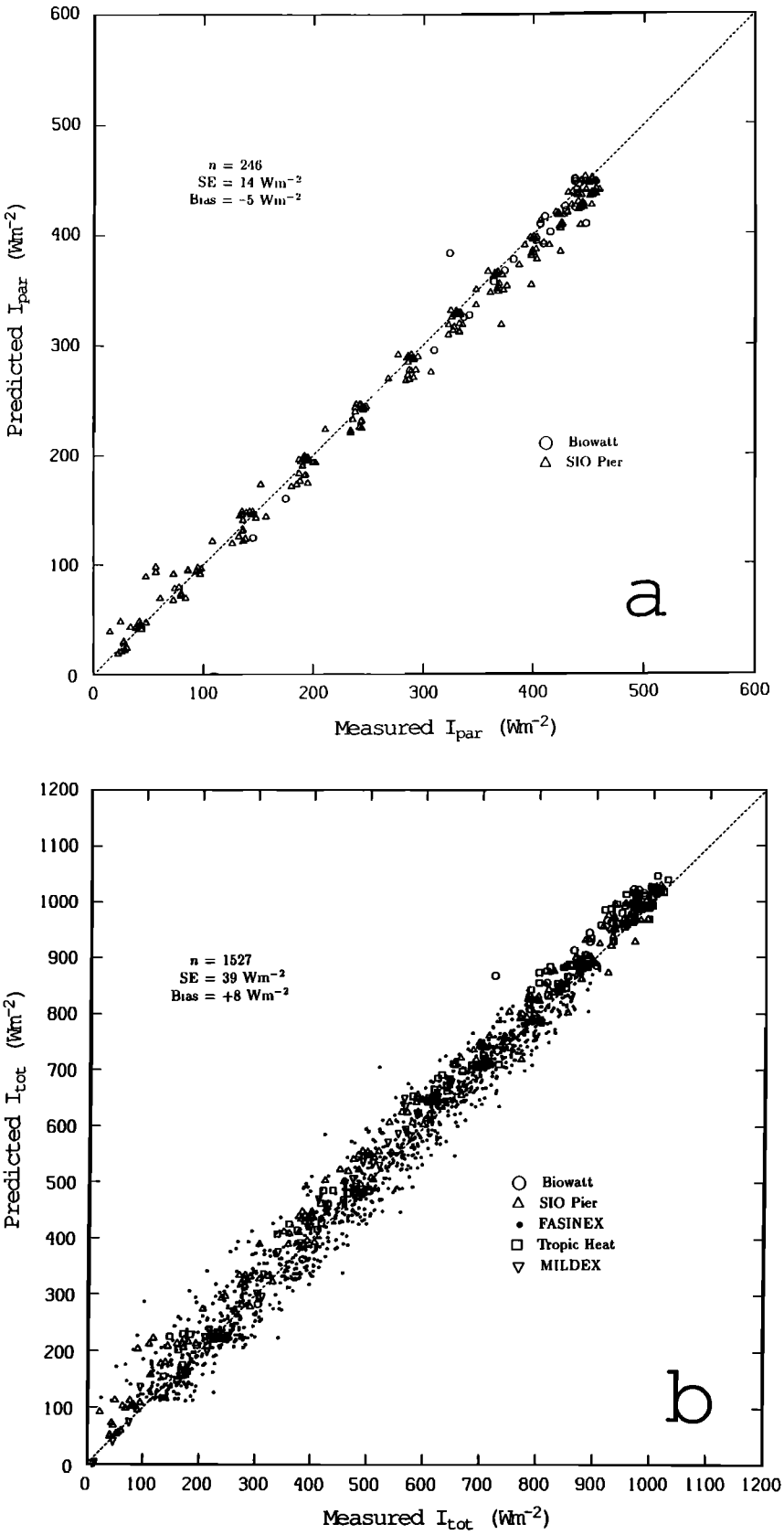

Fig. 3. Scatter plots of (*a*) I_{PAR} and (*b*) I_{tot}. Ordinates are values predicted by the analytical formula using climatological input parameters from Table 3. Abscissas are experimental data.

TABLE 4. Goodness of Fit Statistics (Standard Error and Bias) for Comparisons of Predicted Versus Measured Irradiance Within Each Individual Data Set

Data Set	Number of Points	I_{PAR}, Wm^{-2} SE	I_{PAR}, Wm^{-2} Bias	I_{tot}, Wm^{-2} SE	I_{tot}, Wm^{-2} Bias
Biowatt	22	20	−4	50	+20
SIO pier	224	13	−6	38	+28
MILDEX	42	...	...	32	+23
Tropic Heat	138	...	...	32	+20
FASINEX (all buoys)	1101	...	...	41	+1
Buoy A	183	...	...	38	−0.1
Buoy B	230	...	...	37	−14
Buoy C	192	...	...	33	+4
Buoy D	246	...	...	50	+4
Buoy E	250	...	...	43	+11
All data					
I_{PAR}	246	14	−5	...	...
I_{tot}	1527	...	...	39	+8

cm^{-2} increase in total water vapor amount, for example, reduces I_{tot} by almost 26 W m^{-2} when the sun is at zenith. Each of the parameters would certainly vary widely from the mean on a daily basis, but of the four parameters (aerosol model, visibility, water vapor, and ozone amounts) for which climatological values were used as input to the formula, only the total water vapor amount, because of the spectral position of the water absorption bands, can significantly affect I_{tot} without also changing I_{PAR}. If visibility were actually lower than the climatological average, or ozone content higher, then both the I_{tot} and the I_{PAR} predictions would decrease by a similar proportion. So too would both quantities change proportionately if the aerosol model were actually the opposite from that predicted by published wind vector data.

In contrast, if the actual water vapor concentration were considerably higher than the climatological mean, then the predicted I_{tot} value would decrease, and the predicted I_{par} would remain relatively constant. In fact, if input total water contents were increased by 2.5 g cm^{-2} over the values in Table 3, with all other inputs remaining the same, then, with the exception of the FASINEX buoy sets, the predicted I_{tot} values would be reduced to values very close to the measured data. The bias for Biowatt would drop from +29 to +2 W m^{-2}; that for SIO pier, from +28 to +3 W m^{-2}; that for MILDEX, from +23 to +4; that for Tropic Heat, from +20 to +2 W m^{-2}; and that for FASINEX, from +1 to −16 W m^{-2}. If the maritime aerosol model had been used for FASINEX, then raising the input total water amount by 2.5 g cm^{-2} would have decreased the bias from +17 to 0 W m^{-2}. The same increase in total water of 2.5 g cm^{-2} would affect predicted I_{PAR} values only slightly: for Biowatt, the bias in I_{PAR} would change from −4 to −5 W m^{-2}; for SIO pier, from −6 to −7 W m^{-2}.

TABLE 5. Sensitivity of I_{PAR} and I_{tot} to Model Input Parameters for a 23-km Visibility, US62 Atmosphere Containing Maritime Aerosols

	$\partial I/\partial U_w$, (Wm^{-2}/g cm^{-2})		$\partial I/\partial U_o$, (W m^{-2}/ 10^{-2} atm-cm)		$\partial I/\partial V$, (W m^{-2}/ km)	
	$\theta = 0°$	$\theta = 60°$	$\theta = 0°$	$\theta = 60°$	$\theta = 0°$	$\theta = 60°$
I^*_{PAR}	−0.8	−0.7	−0.3	0.2	0.4	0.3
I_{tot}	−25.9	−14.2	−0.4	−0.3	0.8	0.7

*$I_{PAR} = I_{400-700}$

Two of the five data sets available happen to include surface air temperature and relative humidity data from which total water may be estimated [*Smith*, 1966]. Although Smith's method assumes a typical shape for the vertical profile of water vapor concentration, it provides total water vapor amounts closer to reality than climatological averages, since water vapor is concentrated in the lower atmospheric layers. On the eleven clear days during the SIO Pier experiment for which direct weather observations are available, the total water content, calculated by the method of Smith, was 2.2 ± 0.4 g cm^{-2}, or 22% higher than the climatological mean of 1.8 g cm^{-2}. (Note that the average observed visibility was 26 ± 18 km, essentially the same as the climatological value of 25 km, and that in none of the 11 days were winds observed coming from any direction east of due north or due south, essentially validating the maritime aerosol model predicted by climatologies and weather maps.) Input of the actual observed total water and visibility data into the model for the SIO pier experiment yields an improved fit for both I_{PAR} (bias for the 11 points decreases from −23 to −15 W m^{-2}) and I_{tot} (bias down from +18 to +2 W m^{-2}). For FASINEX, surface air temperature and relative humidity data are available throughout the experiment for four of the five buoys. Calculation of total water amount yields values all lower than the climatological mean of 2.8 g cm^{-2} (Buoy A, 2.5 ± 0.5; buoy B, 2.6 ± 0.6; buoy C, 2.6 ± 0.6; buoy E, 2.5 ± 0.6 g cm^{-2}; overall range of values is 1.2 to 3.6 g cm^{-2}). Input of these means for total water into (6) would certainly yield I_{tot} values higher than those predicted using the climatological water. The predicted I_{tot} values are also higher when the total water is calculated for each individual point and then input into the analytical formula (for buoy A, the bias is changed from −0.1 to +6 W m^{-2}; for buoy B, from −14 to −11 W m^{-2}; for buoy C, from +4 to +5 W m^{-2}; and for buoy E, from +11 to +13 W m^{-2}). Thus the accuracy of the FASINEX prediction is not significantly improved by consideration of actual observations of surface humidity. In view of the observed total water numbers for the SIO pier and FASINEX experiments, there is unfortunately no good reason to believe that total water climatological averages underestimate the actual total water contents for all five of the experiments considered.

5. Summary and Conclusions

A fairly accurate analytical formula (equation (6)) has been presented for computing total and photosynthetically available solar irradiance at the ocean surface under clear skies. The formula is a parameterization of a more complex radiative transfer model [*Tanré et al.*, 1979] and requires inputs of date, solar zenith angle, visibility, aerosol type, and the vertically integrated concentrations of ozone and water vapor. Compared with Tanré et al.'s model, our formula is accurate to 1–2% for solar zenith angles below 75°. It also performs similarly to formulas developed by *Lumb* [1964], *Atwater and Brown* [1974], and *Davies et al.* [1975] for total solar irradiance, but the agreement is better with Lumb's formula for continental aerosols. It is expected, however, that in the case of high aerosol loading (low visibility), (6) will provide more accurate results than Lumb's formula,

since the latter assumes constant aerosol characteristics, leading to overestimations.

Our formula has been tested against actual radiation data taken on board ships and from buoys during five experiments in various oceanic regions. In the comparisons the formula's input parameters were specified from climatological data, since they were not measured on the platforms carrying the radiation instruments. The results of these comparisons indicate a very good agreement between measured and calculated irradiances for both I_{tot} and I_{PAR}. On an hourly time scale, the standard error of estimate is 39 W m^{-2} for I_{tot} and the bias is 8 W m^{-2}, the values being 14 W m^{-2} and -5 W m^{-2} for I_{PAR}, respectively. For all experiments except FASINEX, however, our formula overestimates I_{tot} by 20–30 W m^{-2}. Although part of the discrepancy might originate from errors relating to decoupling gaseous absorption and scattering processes in Tanré's et al.'s model, these cannot account quantitatively for 20–30 W m^{-2}. We did not find convincing evidence that the discrepancy is linked to measurement procedure or instrument calibration or to differences between actual and climatological values for the formula's input parameters. Further work, which may include other comparison experiments (with all the input parameters measured) is therefore required to understand the discrepancy.

Although instruments for directly measuring PAR are being used increasingly, total solar irradiance still remains the radiation parameter most commonly measured at sea. It is therefore worthwhile mentioning that our formula, by giving access to I_{PAR}/I_{tot} theoretically, allows one to convert an I_{tot} measurement into an I_{PAR} estimate. Using the I_{tot} and I_{PAR} data collected during Biowatt and SIO pier experiments, one can even show that I_{PAR}/I_{tot} predicted by our formula is accurate to about 0.03.

Thus we have presented a method to estimate I_{tot} and I_{PAR} which is sufficiently accurate for most applications in biological and physical oceanography. The proposed formula can be used, with the appropriate sets of coefficients, for computing both I_{PAR} and I_{tot}. It also constitutes the only formula presently available to predict PAR at the ocean surface. We have indicated, in the course of comparing our results with in situ data, the type of climatological data sets that can be used as input to the formula. Only the case of clear sky conditions has been addressed in the present study, but the parameterization can be extended to cloudy conditions. In this case, it is generally sufficient to multiply clear sky irradiance by cloud transmittance, T_c. For PAR in particular, the problem is reduced to determining cloud albedo, A_c, since $T_c = 1 - A_c$ (clouds do not absorb in the PAR spectral interval). Determining A_c can be done using satellite radiance measurements in the visible. In fact, estimating PAR from space is of great interest in biological oceanography. Combined with satellite estimates of pigment concentration and sea surface temperature, satellite estimates of PAR give another important parameter in the attempt to assess primary productivity over large oceanic areas and eventually over the global oceans.

Acknowledgments. This work was supported by the Office of Naval Research under contract N00014-84C-0328 (to R.S.), by the National Aeronautics and Space Administration under contracts NAGW-290-3 (to R.S.) and NAGW-851 (to C.G.), and by the California Space Institute. We wish to express our special thanks to Charles R. Booth of Biospherical Instruments, Inc., O. Holm-Hansen and B. Greg Mitchell from the Scripps Institution of Oceanography for providing the SIO Pier radiation measurements, and to all those involved in collecting and reducing the surface radiation data sets. The technical support of Brian Bloomfield and Robert Markworth is gratefully acknowledged.

REFERENCES

Atwater, M. A., and P. S. Brown, Numerical computation of the latitudinal variations of solar radiation from geostationary satellite measurements, *J. Appl. Meteorol.*, *13*, 289–297, 1974.

Baker, K. S., and R. Frouin, Relation between photosynthetically available radiation and total insolation at the ocean surface under clear skies, *Limnol. Oceanogr.*, *32*, 1370–1377, 1987.

Berliand, T. G., Methods of climatological computation of total incoming solar radiation (in Russian), *Meteorol. Gidrol.*, *6*, 9–12, 1960.

Booth, R. C., B. G. Mitchell, and O. Holm-Hansen Development of moored oceanographic spectroradiometer: Final report." *Biosphere Tech. Ref. 87-1*, 69 pp., Biospherical Instrum., San Diego, Calif., 1987.

Davies, J. A., W. Schertzer, and M. Numez, Estimating global solar radiation, *Boundary Layer Meteorol.*, *9*, 33–52, 1975.

Dedieu, G., P. Y. Deschamps, and Y. H. Kerr, Satellite estimation of solar irradiance at the surface of the Earth and of albedo using a physical model aplied to Meteosat data, *J. Clim. Appl. Meteorol.*, *26*, 79–87, 1987.

Deschamps, P. Y., M. Herman, and D. Tanré, Modelisation du rayonnement réfléchi par l'atmosphère et la terre, entre 0.35 et 4μm, *ESA Rep. 4393/80/F/DD(SC)*, 165 pp., Eur. Space Agency, Paris, 1983.

Dickey, T., E. Hartwig, and J. J. Marra, Biowatt: A study of bioluminescence and optical variability in the sea, *Eos Trans. AGU*, *67*, 650, 1986.

Duhaut, P., Influence de l'atmosphère les Mesures Satéllitaires: Simulation et Inversion, Ph.D. thesis, 180 pp., Univ. of Lille, Lille, France, 1985.

Dutsch, H. U. Atmospheric ozone and ultraviolet radiation, in *World Survey of Climatology*, vol. 4, *Climate of the Free Atmosphere*, pp. 383–432, Elsevier, Amsterdam, 1969.

Environmental Data Service, Global monitoring of the environment for selected atmospheric constituents, 1975, technical report, 5 pp., Asheville, N.C., 1977.

Gautier, C., G. Diak, and S. Masse, A simple physical model to estimate incident solar radiation at the surface from GOES satellite data, *J. Appl. Meteorol.*, *19*, 1005–1012, 1980.

Goody, R. M., *Atmospheric Radiation*, 436 pp., Oxford University Press, New York, 1964.

Hay, J. E., and K. J. Hanson, A satellite-based methodology for determining solar irradiance at the ocean surface during GATE, *Bull. Am. Meteorol. Soc.*, *59*, 1549, 1978.

Hill, A. N., J. R. Latimer, A. J. Drummond, and H. Greer, Standardized procedures in the North American continent for the calibration of solar radiation pyranometers, *Sol. Energy*, *10*, 1–11, 1966.

Jerlov, N. G., A simple method for measuring quanta irradiance in the ocean, *Rep.* 24, 10 pp. Inst. Fysisk Oceanogr., Kobenhavns Univ. Copenhagen, 1974.

Jitts, H. R., A. Morel, and Y. Saijo, The relation of oceanic primary production to available photosynthetic irradiance, *Aust. J. Mar. Freshwater Res.*, *27*, 441–454, 1976.

Katsaros, K. B., and J. E. DeVault, On irradiance measurements at sea due to tilt of pyranometers, *J. Atmos. Oceanic Technol.*, *3*, 740–745, 1986.

Kimball, H. H., Amount of solar radiation that reaches the surface of the Earth on the land and on the sea and methods by which it is measured, *Mon. Weather Rev.*, *56*, 393–399, 1928.

Laevastu, T., Factors affecting the temperature of the surface layer of the sea, *Comment. Phys. Math.*, *25*, 1–136, 1960.

Lind, R. J., and K. B. Katsaros, Radiation measurements from R/P *FLIP* and R/V *Acania* during the Mixed Layer Dynamics Experiment (MILDEX), technical report on ONR contract, 44 pp., Dep. of Atmos. Sci., Univ. of Wash., Seattle, 1987.

Lind, R. J., K. B. Katsaros, and M. Gube, Radiation budget components and their parameterisation in JASIN, *Q. J. R. Meteorol. Soc.*, *110*, 1061–1071, 1984.

Lumb, F. E., The influence of cloud on hourly amount of total solar

radiation at the sea surface, *Q. J. R. Meteorol. Soc.*, *90*, 43–56, 1964.

Marra, J., and E. O. Hartwig, "Biowatt: A study of bioluminescence and optical variability in the sea, *Eos Trans. AGU*, *65*, 732–733, 1984.

McClatchey, R. A., R. W. Fenn, J. E. A. Selby, F. E. Vlotz, and J. S. Garine, "Optical properties of the atmosphere, *AFCRL 71-0279 Environ. Res. Pap. 354*, Air Force Geophys. Lab., Hanscom Air Force Base, Mass., 1971.

Meserve, J. M., U.S. Navy marine climatic atlas of the world, vol. 1, North Atlantic Ocean, *Rep. NAVAIR 50-1C-528*, Nav. Weather Serv., Washington, D. C., 1974.

Mosby, H., Verdunstung und Strahlung auf dem Meere, *Ann. Meteorol.*, *64*, 281–286, 1936.

Neckel, H., and D. Labs, The solar radiation between 3300 and 12500 Å, *Sol. Phys.*, *90*, 205–258, 1984.

Niiler, P. P., TROPIC HEAT—A science progress report, in *Further Progress in Equatorial Oceanography: A Report of the U.S. TOGA Workshop on the Dynamics of the Equatorial Oceans*, edited by E. J. Katz and J. M. Witte, pp. 55–69, Nova University Press, Fort Lauderdale, Fla., 1987.

NOAA, Daily weather maps, Public Doc. Dep., U.S. Government Printing Office, Washington, D. C., 1984.

NOAA, Daily weather maps, Public Doc. Div., U.S. Government Printing Office, Washington, D. C., 1985.

Pennington, N. J., and R. A. Weller, FASINEX: Frontal Air-Sea Interaction Experiment: Summaries for FASINEX mooring cruises, *Tech. Rep. WHOI-86-35*, 235 pp., Woods Hole Oceanogr. Inst., Woods Hole, Mass., 1986.

Prabhakara, C., D. A. Short, and B. E. Vollmer, El Niño and atmospheric water vapor: Observations from Nimbus-7 SMMR, *J. Clim. Appl. Meteorol.*, *24*, 1311–1324, 1985.

Reed, R. K., On estimating insolation over the ocean, *J. Phys. Oceanogr.*, *7*, 482–485, 1977.

Simpson, J. J., and C. A. Paulson, Mid-ocean observations of atmospheric radiation, *Q. J. R. Meteorol. Soc.*, *105*, 487–502, 1979.

Smith, R. C., C. R. Booth, and J. L. Star, Oceanographic bio-optical profiling system, *Appl. Opt.*, *23*, 2791–2797, 1984.

Smith, W. L., Note on the relationship between total precipitable water and surface dew point, *J. Appl. Meteorol.*, *5*, 726–727, 1966.

Tanré, D., M. Herman, P. Y. Deschamps, and A. Deleffe, Atmospheric modeling for space measurements of ground reflectances, including bidirectional properties, *Appl. Opt.*, *18*, 3587–3596, 1979.

Tanré, D., C. Deroo, P. Duhaut, M. Herman, J. J. Morcrette, J. Perbos, and P. Y. Deschamps, Effets atmosphériques en télédétection–logiciel de simulation du signal satellitaire dans le spectre solaire," paper presented at the Third International Colloquium on Spectral Signatures of Objects in Remote Sensing, Les Arcs, France, Dec. 16–20, 1985.

Tarpley, J. D., Estimating incident solar radiation at the surface from geostationary satellite data, *J. Appl. Meteorol.*, *18*, 1172–1181, 1979.

Viollier, M., Télédetection des concentrations de seston et pigments chlorophylliens contenus dans l'océan, Ph.D. thesis, 385 pp., Univ. of Lille, Lille, France, 1980.

World Climate Program, Report of the WMO radiation commission of IAMAP meeting of experts on aerosols and their climatic effects, *Rep. WCP 55*, Geneva, 1983.

K. S. Baker, Marine Bio-Optics, Scripps Institution of Oceanography, La Jolla, CA 92093.

R. Frouin, C. Gautier, and D. W. Lingner, California Space Institute, Scripps Institution of Oceanography, La Jolla, CA 92093.

R. C. Smith, Marine Bio-Optics, University of California, Santa Barbara, CA 93106.

(Received November 17, 1988;
accepted January 16, 1989.)